STAT3 mutations correlated with hyper-IgE syndrome lead to blockage of IL-6/STAT3 signalling pathway

JIANXIN HE[1], JIE SHI[1], XIMING XU[1], WENHUA ZHANG[1], YUXIN WANG[1], XING CHEN[1], YUPING DU[1], NING ZHU[1], JING ZHANG[1], QIN WANG[1,*] and JINBO YANG[1,2,*]

[1]*School of Life Science, Lanzhou University, Lanzhou, Gansu 730000, People's Republic of China*

[2]*Department of Cancer Biology, Lerner Research Institute, The Cleveland Clinic Foundation, 9500 Euclid Avenue, Cleveland, OH 44195, USA*

**Corresponding author (Fax, 0086-931-8915350; Email, qwang@lzu.edu.cn; yangjb@lzu.edu.cn)*

Of all the causes identified for the disease hyper-immunoglobulinemia E syndrome (HIES), a homozygous mutation in tyrosine kinase2 (TYK2) and heterozygous mutations in STAT3 are implicated the defects in Jak/STAT signalling pathway in the pathogenesis of HIES. Mutations of STAT3 have been frequently clinically identified in autosomal-dominant (AD) HIES patients' cells, and therefore, the genotype of STAT3 has been associated with the phenotype of HIES. Here, we conducted studies on the functional loss of the seven specific STAT3 mutations correlated with AD-HIES. Using STAT3-null human colon carcinoma cell line A4 cells, we generated seven mutants of STAT3 bearing single mutations clinically identified in AD-HIES patients' cells and studied the functional loss of these mutants in IL-6-Jak/STAT3 signalling pathway. Our results show that five STAT3 mutants bearing mutations in the DNA-binding domain maintain the phosphorylation of Tyr705 and the ability of dimerization while the other two with mutations in SH2 domain are devoid of the phosphorylation of Try705 and abrogate the dimerization in response to IL-6. The phosphorylation of Ser727 in these mutants shows diversity in response to IL-6. These mutations eventually converge on the abnormalities of the IL-6/Gp130/Jak2-mediated STAT3 transactivation on target genes, indicative of the dysregulation of JAK/STAT signalling present in HIES.

[He J, Shi J, Xu X, Zhang W, Wang Y, Chen X, Du Y, Zhu N, Zhang J, Wang Q and Yang J 2012 STAT3 mutations correlated with hyper-IgE syndrome lead to blockage of IL-6/STAT3 signalling pathway. *J. Biosci.* **37** 243–257] **DOI** 10.1007/s12038-012-9202-x

1. Introduction

The complex primary immunodeficiency disease documented as hyper-immunoglobulinemia E syndrome (HIES) (also known as Job's syndrome) is caused by specific genetic mutations that oversensitize the human immune system, rendering the patients susceptible to a spectrum of infections, most commonly *Aspergillus, Staphylococcus aureus* and *Candida albicans* (Minegishi 2009). Since its first discovery as Job's syndrome in 1966, and wherein marked as recurrent, 'cold' and staphylococcal abscesses (Davis *et al.* 1966), cases of HIES have been reported year by year with novel clinic features and genetic underpinnings. Demonstrating markedly elevated serum IgE levels (10 times more than normal level) (Buckley *et al.* 1972), patients with HIES also exhibit a wide range of clinical phenotypes, including connective tissue, skeletal and vascular abnormalities (Grimbacher *et al.* 1999a). Besides, abnormalities of humoral, cellular and phagocytic compartments of the immune system are also observed in HIES patients (Grimbacher *et al.* 2005). The comprehensive analysis of causes of death in HIES highlights the role *Pseudomonas* and *Aspergillus* species play in patients with HIES with cystic lung disease and suggests that HIES patients, if complicated with other diseases, run increased risk of dying (Freeman *et al.* 2007). More than 200 HIES patients have been clinically evaluated and their immunologic features and genetic defects have been analysed, providing invaluable information for full understanding of the pathogenesis of HIES. Based on the etiology and different characteristics, HIES can be subdivided

Keywords. Hyper-IgE syndrome; IL-6; Jak/STAT3 signalling; STAT3 mutation

Published online: 28 April 2012

into two distinct types: autosomal-recessive (AR) HIES and autosomal-dominant (AD) HIES (Minegishi 2009). Multipoint analysis and simulation testing among 44 HIES patients and their 99 relatives (8 having mild form of HIES) confirmed the genetic linkage of HIES to Chromosome4 (Grimbacher *et al.* 1999b). Later on, the identification of genes and genetic mutations involved in the HIES has been extensively pursued. STAT3, DOCK8 and TYK2 have been reportedly associated with HIES and study of these three genetic etiologies is expected to advance the understanding of the pathogenesis of HIES (Freeman and Holland 2010). However, of the many genomic loci involved in the sporadic and AD-HIES, STAT3 mutation has been established as the predominant cause (Holland *et al.* 2007; Minegishi *et al.* 2007), and thus the defect of Janus kinase-signal transducer and activator of transcription (Jak/STAT) signalling pathway is universally implicated in the pathogenesis of AD-HIES.

The investigation in this pathway has already shed light on a number of diseases ranging from immunodeficiencies to hematological malignancies since the Jak and STAT proteins were associated in the gene activation pathway in 1994 (Darnell *et al.* 1994). Jak/STAT signalling pathway comprises sufficiently diverse and conserved proteins of Jak family (Jak1, Jak2, Jak3, and Tyk2) and STAT family (STAT1, 2, 3, 4, 5a, 5b and 6) which mediate the signal transduction and are in turn activated and tuned by various ligands and three major classes of negative regulators: SOCS, PIAS and PTPs (Darnell 1997; Schindler *et al.* 2007). Jak proteins and STAT proteins play pivotal roles in structuring and modulating the Jak/STAT signalling pathway. STAT3, when activated by tyrosine phosphorylation in response to epidermal growth factor (EGF) and/or interleukin-6 (IL-6), dimerizes via its reciprocal phosphotyrosine-SH2 domain interactions and translocates into the nucleus, poising to activate transcription of target genes with promoters containing GAS element (TTCNNNGAA) (Seidel *et al.* 1995; Zhong *et al.* 1994). Canonically, Jak1 and Jak2 that are activated by IL-6 or/and EGF bind to and phosphorylate gp130 on tyrosine to produce a phosphotyrosine docking site for STAT3 (Heinrich *et al.* 1998). STAT3 is subsequently Tyr705- and Ser727-phosphorylated by Jaks within its carboxyl-terminal region (Schuringa *et al.* 2000). Upon Tyr705 phosphorylation, STAT3s form stable dimers and translocate into the nucleus, ensuing the expression of downstream genes. However, recent study found that dimethylation at Arg109 by SET9 and demethylation by LSD1 as STAT3s bind to the promoters mediate the transcription of target genes (Yang *et al.* 2010). The direct sequencing analysis of mutations of STAT3 in AD-HIES patients' cells reveals that the mutations occur collectively in the DNA-binding domain, SH2 domain and transactivation domain, where five hot spots have been identified: R382, F384, R423, V463 and V637 (Holland *et al.* 2007; Minegishi *et al.* 2007; Renner *et al.* 2007). Later on, H332Y in the DNA-binding region was identified as a novel mutation that results in the loss of function of STAT3 and leads to the HIES phenotype (Jiao *et al.* 2008). R335W, K340N, T341L, V343L, Q469H, T620A, S636F, E638G, P699Δ, V713L as well as defective mRNA spicing have also been implicated in the HIES and the analysis of the mutants cells suggests a defective phosphorylation in mutants harbouring mutations within SH2 domain (Renner *et al.* 2008). Recently, it has been reported that impaired differentiation of Th17 cells in AD-HIES patients, which is due to mutation of STAT3 in DNA-binding domain and SH2 domain, dramatically leading to the susceptibility of HIES patients to various recurrent infections (Ma *et al.* 2008; Milner *et al.* 2008). Additionally, secretion of immunoglobulin E in HIES patients, which is induced by IL-21, has been demonstrated to be STAT3 dependent (Avery *et al.* 2008). Furthermore, a novel mutation G342D from HIES patient, which is located in DNA-binding domain of STAT3, has been demonstrated to lose its DNA-binding ability and fail to induce the expression of RORγ, finally leading to the HIES phenotype (Papanastasiou *et al.* 2010). HIES patients with positive STAT3 mutation exhibited reduced Tyr705 phosphorylation of STAT3 in response to cytokine stimulation (Al Khatib *et al.* 2009), and SH2 domain mutation of STAT3 from HIES has defective phosphorylation in Tyrosine 705 residue (Renner *et al.* 2008).

In this study, by using the site-directed mutagenesis method and Lenti-virus expression system, we generated with STAT3-null human colon carcinoma cell line A4 cells seven mutants of STAT3 bearing single mutations in DNA-binding and SH2 domains. These mutations are highly conserved and have been clinically manifested in the HIES patients' cells (Grimbacher *et al.* 1999b; Holland *et al.* 2007; Jiao *et al.* 2008). H332Y, R382W, R382Q, F384S and R423Q are located in the DNA-binding domain whereas S611N and F621V are located in the SH2 domain. We evaluate the phosphorylation status of STAT3, dimerization and nuclear localization, DNA binding ability, and transcriptional activation of target genes in these mutant cells in response to IL-6. Our results show that the IL-6-Jak/STAT3 signalling pathway in the all mutants has been greatly affected, leading to an aberrant expression pattern of STAT3 target genes.

2. Materials and methods

2.1 *Cell culture and reagents*

The human colon carcinoma cell line DLD1 cells were obtained from the American Type Culture Collection and the

STAT3-null human colon cancer cell line A4 cells were provided as a gift by George R Stark's laboratory (Yang *et al.* 2010). The cells were grown in McCoy's 5A medium with L-glutamine (HyClone) supplemented with 10% FBS and were incubated at 37°C in a humidified atmosphere of 5% CO_2 unless otherwise indicated. Antibodies against STAT3, Y705-phosphoryl STAT3 (pY705-STAT3), S727-phosphoryl STAT3 (pS727-STAT3), GAPDH, Histones3 and HA were purchased from Cell Signalling Technology. Anti-Flag M2 antibody and Puromycin were purchased from Sigma-Aldrich (St. Louis, USA). Peroxidase-Conjugated AffiniPure Goat Anti-Rabbit IgG (H+L) and Peroxidase-Conjugated AffiniPure Goat Anti-Mouse IgG (H+L) were purchased from ZSGB-Bio (Beijing, China). Alexa Fluor® 488 $F(ab')_2$ fragment of goat anti-rabbit IgG (H+L) was purchased from Invitrogen US. Recombinant Human sIL-6 Rα was purchased from PEPROTECH (New Jersey, USA). GenEscort^{TM} Transfection Reagent was purchased from Wisegen Biotechnology Corporation (Nanjing, China). Lipofectamine transfection reagent and Sepharose A beads for Co-IPs were purchased from Invitrogen (Carlsbad, USA).

2.2 *Plasmid construction and virus infection*

The H332Y, R382W, R382Q, F384S, R423Q, S611N and F621V mutations of STAT3 were generated from human wild-type STAT3 cDNA by using the QuikChange II Site-Directed Mutagenesis Kit (Stratagene). The design of the primers and the sequence is described in table 1. The pLV-puro-sv40, pMD-2 G, pCMV-dr8.74 vectors were provided by George R. Stark's laboratory (Lener Institute, Cleveland). The expression vectors of STAT3 mutants were constructed by inserting the cDNA of each mutant sequence into the XhoI site of the pLV-puro-sv40 vector. To obtain infectious lenti-virus stocks, all the three constructs were transfected into HEK293T cells using lipofectamine and cells were kept growing in supernatant medium. After 48 h, cells were collected and were used to infect A4 cells for 2 days. Clones of stable transfection were selected and proliferated in medium supplemented with 5 μg/mL of puromycin for 10–15 days. HA-tagged sequences of STAT3 mutations were inserted into pEGFP-N1 between XhoI and HindIII restriction sites and the plasmids were transiently transfected into A4 cells for expression of proteins.

2.3 *Western blot analysis*

Cells grown up to 80% confluence in 100 mm dishes were harvested and washed once with PBS. The cell pellets were lysed by ultrasonication for 15 s on ice in 200 μL RIPA lysis buffer containing 50 mM Tris–HCl (pH 7.5), 150 mM NaCl, 1% NP-40, 0.5% DOC, 0.1% SDS, 5 mM EDTA, 1 mM EGTA, 20 mM NaF, 2 mM NaOrthovanaclate and Protease Inhibitor Cocktail (Roche). Extracts containing equal quantities of proteins, determined by the Bradford method (Bio-Rad, Hercules, CA), were separated by SDS-PAGE (12% acrylamide) and transferred to polyvinylidenedifluoride membranes (Millipore, Bedford, MA). Membranes were probed with antibodies specific for S727-phosphoryl STAT3, Y705-phosphoryl STAT3, STAT3, GAPDH, Histone3, HA and Flag, respectively. Horseradish peroxidase–coupled goat anti-rabbit or anti-mouse immunoglobulin was used for visualization, employing the enhanced chemiluminescence Western detection system (Perkin-Elmer Life Sciences, Boston, USA).

2.4 *Transient transfection*

A4 cells expressing Flag-tagged mutants of STAT3 were transiently transfected with reconstructed pEGFP-N1 vectors inserted by HA-tagged mutants of STAT3 between XhoI and HindIII sites. Cells grown up to 50% confluence in 100 mm dishes were co-cultured with mixture of DNA and Wisegen Transfection Reagent (1ug DNA: 2ul Reagent) for 3 h. Then, the cell culture medium was replaced with fresh McCoy's 5A medium supplemented with 10% FBS and cells were

Table 1. Sequence information of mutant primers

	Forward primer sequence(5′-3′)	Reverse primer sequence (5′-3′)
H332Y	AGCCCTGCATGCCCATGTATCCTGACCGGCCCCTCG	CGAGGGGCCGGTCAGGATACATGGGCATGCAGGGCT
R382W	GCTCTCAGAGGATCCTGGAAATTTAACATTCTGGG	CCCAGAATGTTAAATTTCCAGGATCCTCTGAGAGC
R382Q	GCTCTCAGAGGATCCCAGAAATTTAACATTCTGGG	CCCAGAATGTTAAATTTCTGGGATCCTCTGAGAGC
F384S	GCTCTCAGAGGATCCCGGAAATCTAACATTCTGG	CCAGAATGTTAGATTTCCGGGATCCTCTGAGAGC
R423Q	GGGAATGGGGGCCAAGCCAATTGTGATGC	GCATCACAATTGGCTTGGCCCCCATTCCC
S611N	GCTAAGATTCAATGAAAGCAGCAAAGAAGGAGGCG	CGCCTCCTTCTTTGCTGCTTTCATTGAATCTTAGC
F621V	GCAAAGAAGGAGGCGTCACTGTCACTTGGGT	ACCCAAGTGACAGTGACGCCTCCTTCTTTGC

kept growing for 36 h. Prior to co-immunoprecipitation, cells were treated with 50 ng/mL IL-6 for 2 h.

2.5 *Co-immunoprecipitations*

The protocol provided by Sigma-Aldrich was followed, with slight modifications. For immunoprecipitation of STAT3 from A4 cells expressing either wild-type STAT3 or the mutants, cells cultured in 100 mm dishes were harvested and lysed in IP buffer containing 50 mM Tris–HCl, pH 8.0, 150 mM NaCl and 1% Nonidet P-40. Monoclonal anti-FLAG M2 antibody was used to bind to Flag-tagged STAT3. Sepharose A beads were used to bind to the proteins–antibody complex, which were subsequently mixed with 5× SDS sample loading buffer for analysis in 12% SDS/PAGE gels.

2.6 *Fluorescence microscopy*

Cells were seeded on glass cover slips and were grown to 50% confluency. Cells were initially fixed in 4% paraformaldehyde for 20 min and then in absolute methanol for 5 min at room temperature, followed by the treatment with blocking buffer containing PBS (1×), 0.3% Triton X-100 and 10% Bovine Serum Albumin Fraction V for 10 min. STAT3 signals were detected with rabbit anti-human STAT3 and were visualized by Alexa Fluor® 488 F goat anti-rabbit (greenfluorescent) secondary antibodies (Invitrogen). The VECTASHIELD MOUNTING MEDIUM with DAPI (Vectot Laboratories, USA) was added for monitoring the nuclear localization. Images were captured with a Zeiss Axioskop fluorescence microscope and presented by PHOTOSHOP (Adobe System Inc.).

2.7 *Isolation of cytoplasmic fraction and nuclear fraction*

The cytoplasmic fraction and nuclear fraction were prepared by using the method as follows: Briefly, cells growing in 150 mm dishes were cultured to the indicated confluence for treatment with IL-6 for 2 h. Then, cells were collected by centrifugation at 2000*g* for 2 min at 4°C and washed twice with ice-chilled PBS added with protease and phosphatase inhibitor. Cells were re-suspended in 5 volumes of ice-chilled nuclear buffer containing 10 mM Hepes, pH7.5, 1.5 mM $MgCl_2$, 10 mM KCl, 0.5% NP40 added with protease and phosphatase inhibitor. Cells were swollen on ice for 30 min and broken by the use of a Dounce homogenizer for 90 s. The lysate was centrifuged at 12,000*g* for 5 min. The supernatant contains cytoplasmic proteins and was directly transferred to a new tube; the pellet containing nuclear proteins was further washed by centrifugation as described for the lysate. The pellet was lysed by ultrasonication for 15 s on ice in 100 μL RIPA lysis buffer and then centrifuged at 14,000*g* for 10 min at 4°C. The nuclear proteins are in the supernatant. Western blot analysis was performed by loading protein samples representing equal quantity of cells.

2.8 *Electrophoretic mobility shift analysis*

Cells were lysed in buffer containing 10 mmol/L HEPES (pH 7.9), 60 mmol/L KCl, 1 mmol/L EDTA, 0.1 mmol/L EGTA, 0.075% NP-40, 1 mmol/L Na_3VO_4, 5 mmol/L NaF, 1 mmol/L DTT, 1 mmol/L phenylmethanesulfonylfluoride, Protease Inhibitor Cocktail (Roche) and Phosphatase Inhibitor Cocktail (Roche). After incubation for 30 min on ice, the debris was removed by centrifugation at 16,000*g* at 4°C for 30 min. Protein concentrations were determined by the Bradford method. Binding reactions buffer contained 1 L of lysate (5–10 g of protein), 1 μL of sonicated salmon sperm DNA (0.5 mg/mL), 1.4 μL of 5 shift buffer [100 mmol/L HEPES (pH 7.9), 200 mmol/L KCl, 30 mmol/L $MgCl_2$, 0.5% NP40, 5 mmol/L DTT and 5 mmol/L phenylmethylsulfonylfluoride], 1.5 μL of bovine serum albumin (1 mg/mL), 3.8 μL of H_2O, 0.3 μL of probe, end-labelled with T4 polynucleotide kinase and [^{32}P]-ATP. The probe was the GAS consensus sequence (top strand 5′-CGATTCCTGG AACTGCGCGG-3′) from human *socs3* promoter. 10^4 dpm of labelled probe was used in each binding reaction. Protein–DNA complex was separated by electrophoresis in Gel composed of 4% acrylamidebisacrylamide (29:1), 0.5× TBE (45 mmol/L Tris–HCl, 44 mmol/L boricacid, and 1 mmol/L EDTA), and 5% glycerol.

2.9 *Quantitative real-time PCR*

Total RNAs were extracted from cells expressing STAT3 treated or untreated with IL-6, using RNAprep pure Cell Kit (TIANGEN, China). cDNA was synthesized using EasyScript Reverse Transcriptase under priming of oligo$(dT)_{18}$ (TransGen, US). Real-time PCRs were performed by CFX96 Real-Time PCR Detection System (Bio-Rad) using the SYBR® Premix Ex Taq^{TM} II kit (TaKaRa, Inc.). The data was normalized to GAPDH reference. The design of primers is described in table 2.

2.10 *Statistical analysis*

In quantitative real-time PCR assay, experiments were performed in quadruplicate, and data were expressed as means±SE. Statistical comparison between groups was presented using one-way ANOVA. *$P<0.05$, and **$P<0.01$ was considered to be statistically significant.

Table 2. Sequence information in quantitative real-time PCR

	Forward primer sequence(5′-3′)	Reverse primer sequence (5′-3′)
SOCS3	CAGGAATGTAGCAGCGATGGAA	CCTGTCCAGCCCAATACCTGA
c-FOS	CTACCACTCACCCGCAGACTCCTT	CACTGCAGGTCCGGACT
c-JUN	TCCTGAAACAGAGCATGACC	CCGTTGCTGGACTGGATTAT
GAPDH	TGGCAAATTCCATGGCAC	CCATGGTGGTGAAGACGC

2.11 *Molecular modelling*

STAT3(1–770)–DNA complex structure was modelled by Modeller (http://salilab.org/modeller/). Template structures were STAT3–DNA complex (PDB ID: 1BG1) and STAT1 (PDB ID: 1YVL). Binding affinity between STAT3 and DNA was caculated by FoldX molecular design toolkit (Guerois *et al.* 2002; Schymkowitz *et al.* 2005), using a GAS sequence (top strand 5′-TCGACATTTCCCGTAAATC-3′) from human *c-fos* promoter. The free energy is calculated by FoldX force field with the following equation:

$$\Delta G = \Delta G_{vdw} + \Delta G_{solvH} + \Delta G_{solvP} + \Delta G_{hbond} + \Delta G_{wb} + \Delta G_{el} + \Delta G_{kon} + T\Delta S_{mc} + T\Delta S_{sc} + \Delta G_{clash}$$

where ΔG_{vdw} is the van der Waals term; ΔG_{solvH} and ΔG_{solvP} are the solvation energy of apolar and polar atom groups; ΔG_{hbond} is the term of hydrogen bonds; ΔG_{wb} is the stabilizing free energy by water; ΔG_{el} is the electrostatic contribution; ΔG_{kon} is the electrostatic contributions of interaction atoms from two molecules; $T\Delta S_{mc}$ and $T\Delta S_{sc}$ are dipole and entropy cost respectively ; ΔG_{clash} is taken into account of atoms steric overlaps. In this study, T is set to 298 K during structure repairing and energy calculation.

3. Results

Using STAT3-null A4 cell line, we generated seven STAT3 mutants bearing single mutations correlated with HIES. H332Y, R382W, R382Q, F384S, R423Q are mutations in STAT3 DNA-binding domain and the other two, S611N and F621V, are within SH2 domain (figure 1A). The expression levels of the STAT3 proteins were evaluated in cells expressing either wild-type STAT3 or individual STAT3 mutants. Compared to the expression level of wild-type STAT3 in parental DLD1 cells, all the expression levels of Flag-tagged STAT3 in A4 cells were increased by 10-fold, as judged by densitometric quantitation of the bands (figure 1B). The pooled cells grew at rate very similar to those of parental DLD1 cells. The phosphorylation status of Tyr705 and Ser727, the dimerization, the nuclear localization and transactivation effect on target genes in all the mutants of STAT3 have been evaluated, leading to conclusion that the IL-6-Jak/STAT3 signalling pathway in all the seven mutants has been essentially blocked.

3.1 *Mutations in SH2 domain of STAT3 lead to the loss of Tyr705 phosphorylation but not Ser727 phosphorylation in response to IL-6*

The phosphorylation status of STAT3 in each mutant was examined by Western blot analysis. STAT3-null A4 cells and A4 cells expressing either wild-type STAT3 or individual mutants were untreated or treated with IL-6 prior to the Western blot analysis. Tyr705 phosphorylation is only detected with Y705-phosphoryl STAT3 antibody in wild-type STAT3, H332Y, R382W, R382Q, F384S and R423Q (mutations in DNA-binding domain) mutants cells only after treatment with IL-6, whereas it is neither detected in S611N and F621V (mutations in SH2 domain) mutants cells after treatment with IL-6 nor in all the cells in absence of treatment with IL-6 (figure 2A). The expression of the STAT3 remains unaffected during the treatment with IL-6 in all cells except STAT3-null cells as judged by the Western blot analysis of STAT3 and GAPDH (figure 2A). These results are consistent with previous work (Minegishi *et al.* 2007; Renner *et al.* 2008) and highlight the importance of SH2 domain in maintaining Tyr705 phosphorylation. Strikingly, the overall phosphorylation status of Ser727 is lower than that of Tyr705 in DNA-binding domain mutants STAT3 (figure 2B). However, in response to IL-6 stimulation, Ser727 phosphorylation of F384S and R423Q increases, Ser727 phosphorylation of R382Q and S611N raises a little as wild-type STAT3 does. Ser727 phosphorylation of H332Y and F621V seem unaffected, while that of R382W goes down, in response to IL-6 stimulation (figure 2B). These results indicate that regulation of Ser727 phosphorylation is independent of SH2 domain of STAT3 in these mutant cells.

3.2 *Mutations in SH2 domain lead to the loss of dimerization of STAT3*

Based on the observation of impaired phosphorylation status of STAT3 in the mutants cells, we further evaluated the effect of the mutations on the dimerization of STAT3 via transfecting the HA-tagged STAT3 into Flag-tagged STAT3 mutants cells.

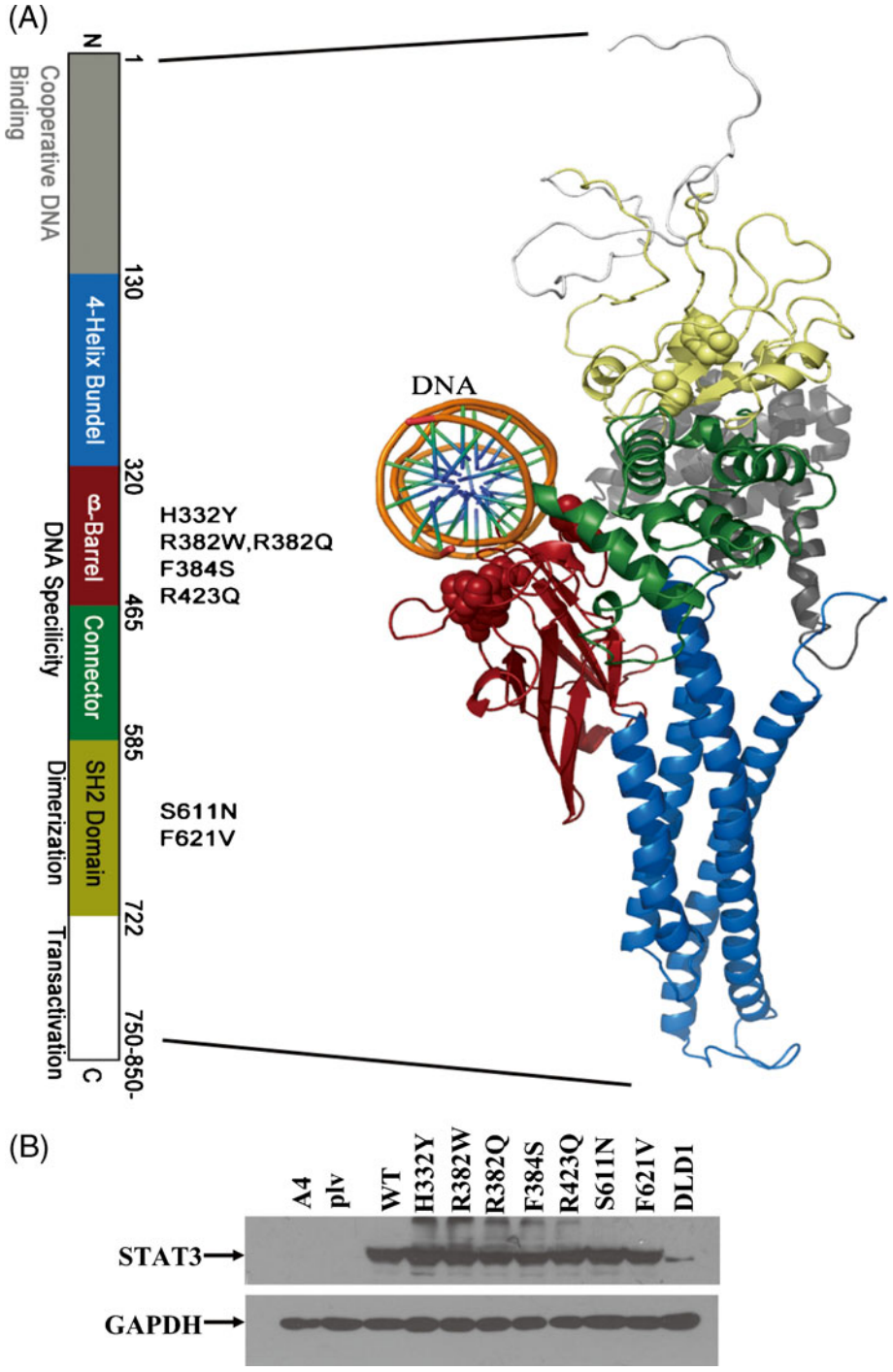

Figure 1. Construction of the mutant cell lines. (**A**) Structure model of STAT3-DNA complex and mutation sites. The areas of the same colour in the left and right pictures were the same domain of STAT3. All the mutant sites we studied in this work have been marked in the left picture and drawn in sphere type in the right picture. (**B**) Construction of STAT3-expressing cell lines. A4 cell was infected by lenti-virus packing mutant STAT3 in DNA-binding domain or SH2 domain for 2 days and the stably infected cell lines were selected with 5 μg/mL puromycin for 10 days. Whole cell extracts were prepared, and Western blot analysis was conducted. pLV was the control representing protein from infected cell by lenti-virus carrying nothing.

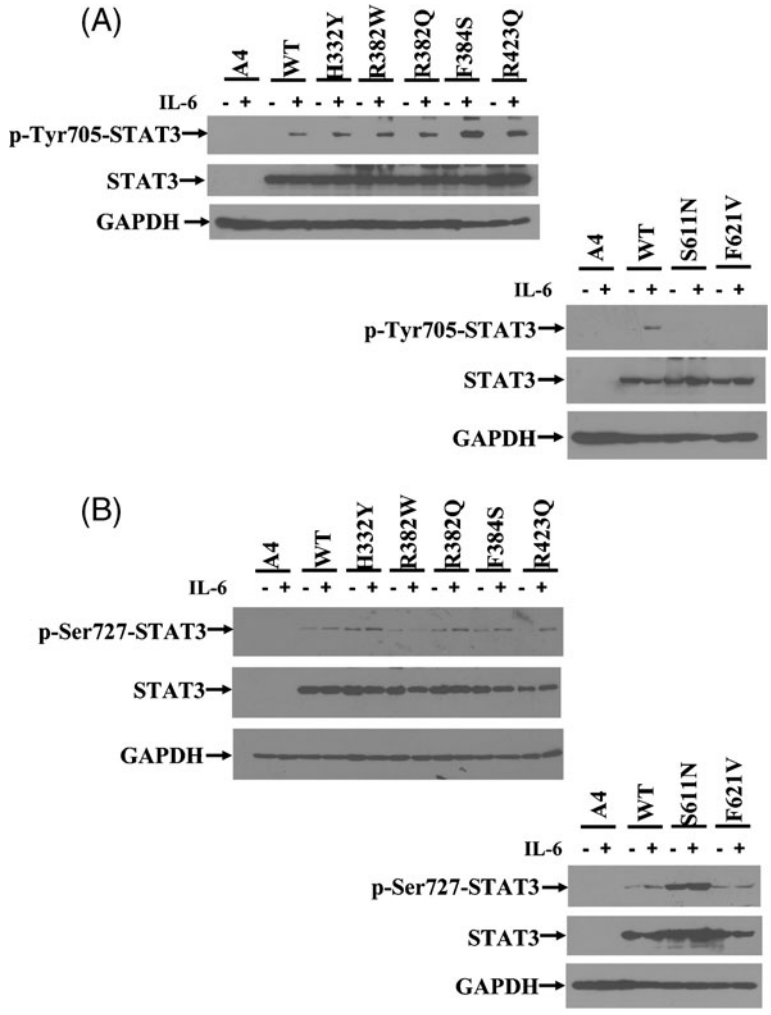

Figure 2. Tyrosine 705 and serine 727 phosphorylation of STAT3 mutants were different in response to IL-6. (**A**) p-Tyrosine 705 and total STAT3 proteins level of mutant STAT3 in constructed cell lines. Cells were untreated or stimulated with IL-6 for 2 h, and whole cell extracts were prepared for Western blot analysis. (**B**) p-Serine 727 and total STAT3 proteins level of mutant STAT3 in constructed cell lines.

Co-immunoprecipitation analysis was performed after cells were treated with IL-6. H332Y, R382W, R382Q, F384S and R423Q mutants of STAT3 (mutations in DNA-binding domain) demonstrate an unaffected dimerization while S611N and F621V mutants (mutations in SH2 domain) fail to form dimmers, in comparison to the wild-type STAT3 (figure 3). Thus, it is manifested that the two mutations within the SH2 domain abrogate the ability of dimerization of STAT3.

3.3 *Nuclear localization of STAT3 with the mutants bearing mutations in both DNA-binding domain and SH2 domain*

Since dimerization is one of the key events for STAT3 to function properly as a transcriptional factor, we subsequently explored the nuclear importing abilities of STAT3 mutants. Immunofluorescence analysis on the cellular localization of STAT3 shows a universal distribution of STAT3 in both cytoplasm and nucleus of cells either untreated or treated with IL-6 (figure 4A, B). Western blot analysis on the cellular localization of STAT3 also demonstrates a universal presence of wild-type STAT3 and all mutant STAT3 in cytoplasm and nucleus, while Tyr705-phosphorylated STAT3 mainly locate in nucleus (figure 4C), in accordance with previous report that nuclear importing of STAT3 is independent of tyrosine phosphorylation and SH2 domain (Liu *et al.* 2005). Interestingly, a little phosphorylation level of Tyr705 in H332Y mutant STAT3 is observed in cytoplasm in response to IL-6 (figure 4C).

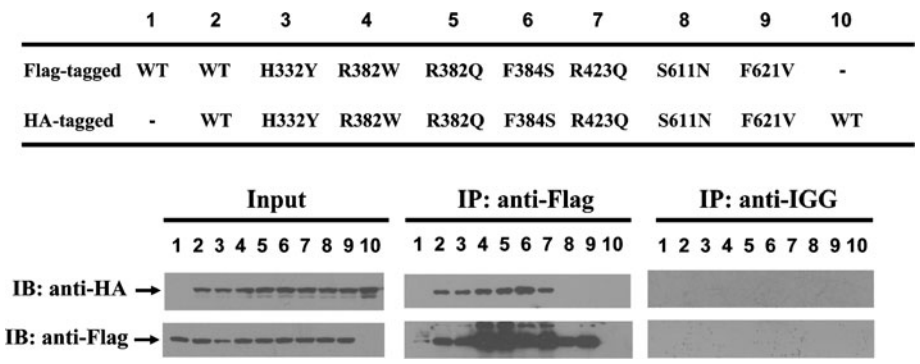

Figure 3. Mutant STAT3 dimerization. All A4 cell lines expressing Flag-tagged STAT3 mutants were transiently transfected with pEGFP-N1 vectors containing HA-tagged mutant STAT3. 36 h after transfection, cells were stimulated with IL-6 for 2 h. Whole cell lysis for Co-immunoprecipitations were prepared, and Co-IPs were performed.

3.4 *Mutations in DNA-binding domain and SH2 domain of STAT3 exhibit an aberrant transactivation of STAT3 target genes*

The impairment to the DNA-binding ability due to heterozygous STAT3 mutation has been reported in HIES patients' cells when treated with IFNα (Minegishi *et al.* 2007) and IL-6 (Papanastasiou *et al.* 2010). To determine the DNA-binding ability of STAT3 with mutations frequently correlated with HIES, electrophoretic mobility shift assay (EMSA) was performed with an oligonucleotide harboring the GAS consensus sequence (5′-CGATTCCTGGAA CTGCGCGG-3′) from the human *socs3* promoter. It shows that mutations in H332Y, R382W, R382Q, F384S, R423Q, S611N and F621V have abrogated the DNA-binding abilities of STAT3 homo-dimer (figure 5A). Upon these findings, we further analysed the binding affinity of DNA to wild-type STAT3 and H332Y, R382Q, R382W, F384S and R423Q STAT3 mutations located in DNA-binding domain (figure 5B–G). Variation in interaction binding energy ($\Delta\Delta G_{kd}$) due to mutations H332Y, R382Q, R382W are 1.64 kcal/mol, 0.82 kcal/mol, 1.49 kcal/mol respectively, which shows binding affinity for those three mutants is decreased. These results together indicate that STAT3 mutations in DNA-binding domain and SH2 domain correlated with HIES eventually attenuate the interaction between STAT3 and promoter sequences of target genes.

To examine the exact effect of the mutations of STAT3 on transcription of STAT3 target genes, we stimulated the wild-type STAT3 cells and mutant cells with IL-6 and examined the relative mRNA expression of *socs3*, *c-fos* and *c-jun*. The results show that expression of *socs3* was totally inhibited in all the STAT3 mutant cells (figure 6A) while the expression of *c-fos* and *c-jun* were reduced to a variable extent (figure 6B and C). These results manifest these STAT3 mutations finally lead to the blockage of IL-6/STAT3 signalling pathway.

4. Discussion

In this study, we have shown that HIES-correlated mutations of STAT3 block the IL-6-Jak/STAT3 signalling pathway, leading to an aberrant transactivation of STAT3 target genes. The dominant-negative heterozygous missense mutations and in-frame deletions in DNA-binding and SH2 domains of STAT3 have been reported as the major cause of HIES (Holland *et al.* 2007). In the present study, we only focused on the functional loss of STAT3 mutations clinically correlated with HIES. STAT3 mutations in R382W, R382Q, F384S, R423Q, S611N and F621V in this study have high NIH clinical scores (>60 points) (Holland *et al.* 2007) and mutation in H332Y is a novel mutation in the STAT3 DNA-binding domain reported in HIES patients (Jiao *et al.* 2008). Previous work has reported that STAT3 bearing R382W mutation but not V637M can be phosphorylated on Tyr705 in Cos-7 cells in response to the stimulation of EGF (Renner *et al.* 2008). The Western blot analysis in our study shows that mutations in SH2 domain of STAT3 lead to the loss of Tyr705 phosphorylation, while mutations

Figure 4. Distribution of Tyr705 phosphorylated STAT3 mutants in ▶ nucleus and cytoplasm in response to IL-6. (**A**–**B**) Immunofluorescence. A4 cell line expressing STAT3 mutants were grown on cover slips to 20–30% confluence and then stimulated with IL-6 for 4 h, followed by staining with primary antibodies directed against STAT3. Following staining with DAPI (blue nuclear stain) and fluorescent secondary antibodies against STAT3 (green), the cells were examined by confocal microscopy ((**A**), 20×; (**B**), 100×). (**C**) Western blot analysis: A4 cells expressing wild-type or mutant STAT3 were untreated or stimulated with IL-6 for 2 h. Cytoplasmic and nuclear fractions representing equal numbers of cells were separated by electrophoresis and analysed by Western blot.

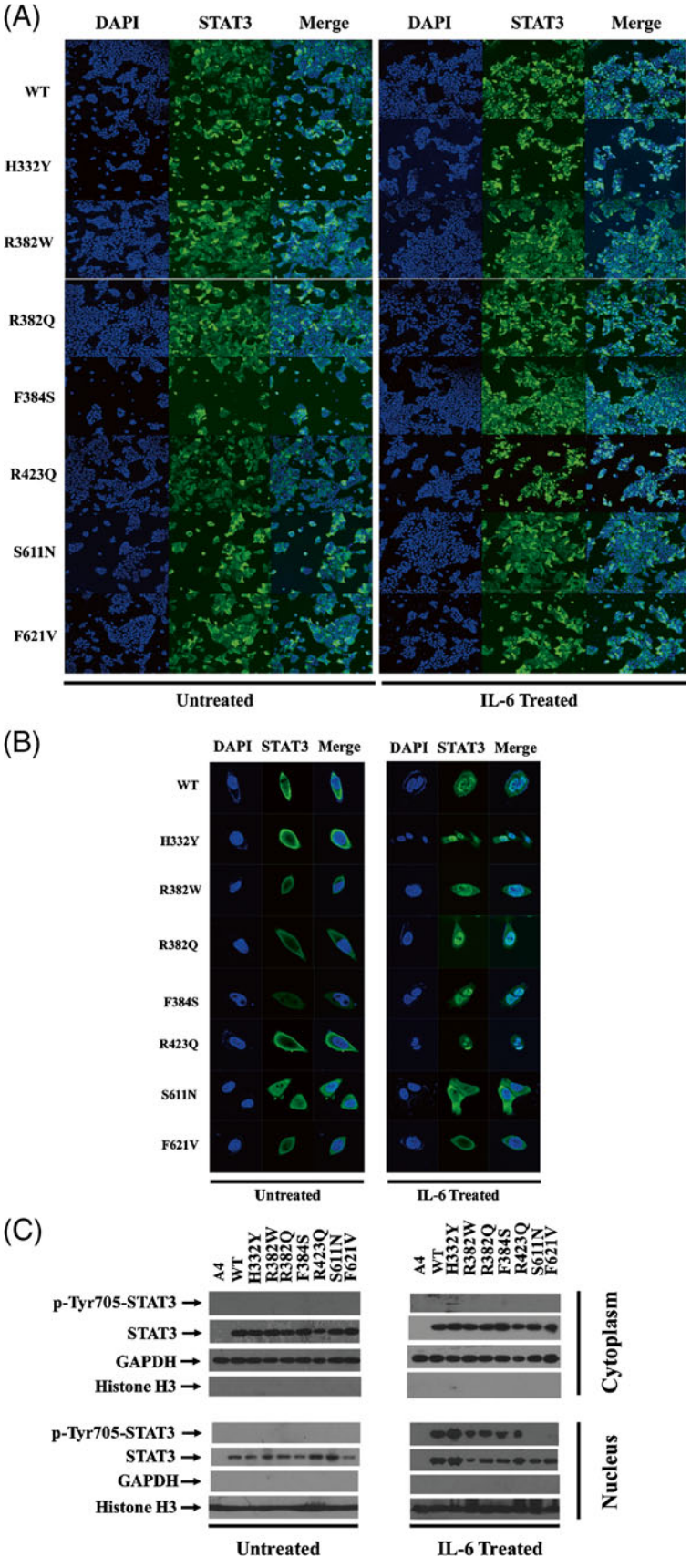
(A)
DAPI
STAT3
Merge
DAPI
STAT3
Merge
WT
H332Y
R382W
R382Q
F384S
R423Q
S611N
F621V
Untreated
IL-6 Treated
(B)
DAPI STAT3 Merge
DAPI STAT3 Merge
WT
H332Y
R382W
R382Q
F384S
R423Q
S611N
F621V
Untreated
IL-6 Treated
(C)
A4
WT
H332Y
R382W
R382Q
F384S
R423Q
S611N
F621V
p-Tyr705-STAT3
STAT3
GAPDH
Histone H3
Cytoplasm
Nucleus
Untreated
IL-6 Treated

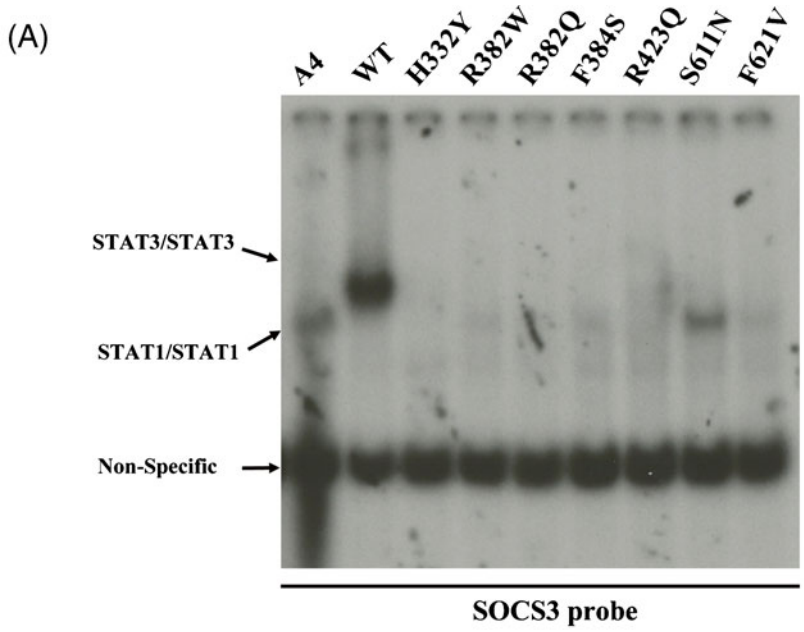
(A)
A4
WT
H332Y
R382W
R382Q
F384S
R423Q
S611N
F621V
STAT3/STAT3
STAT1/STAT1
Non-Specific
SOCS3 probe

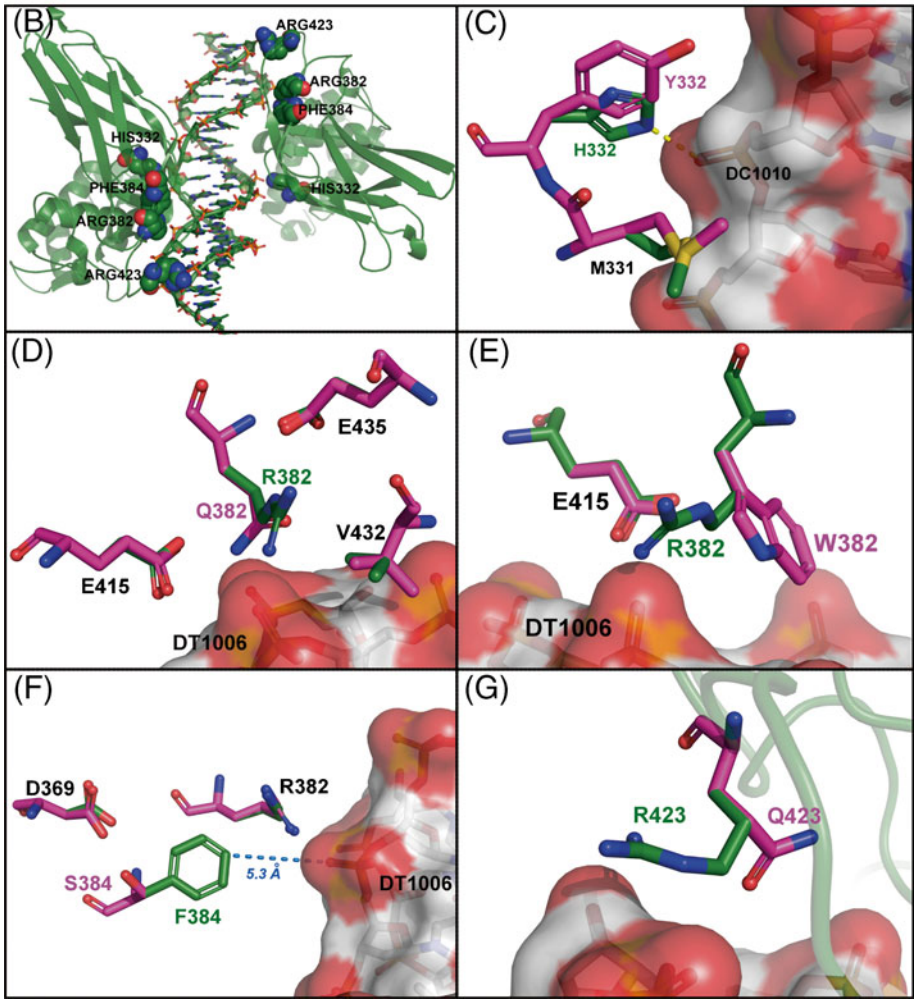
(B)
ARG423
ARG382
PHE384
HIS332
PHE384
HIS332
ARG382
ARG423
(C)
Y332
H332
DC1010
M331
(D)
E435
R382
Q382
V432
E415
DT1006
(E)
E415
R382
W382
DT1006
(F)
D369
R382
S384
5.3 Å
F384
DT1006
(G)
R423
Q423

◀ **Figure 5.** DNA-binding abilities of STAT3 mutants are diminished. (**A**) Electrophoretic mobility shift assay (EMSA). Cells were stimulated with IL-6 for 2 h, and whole cell extracts were prepared. Aliquots containing equal amounts (10 μg) of each extract were analysed by EMSAs. A ^{32}P-labelled GAS consensus sequence derived from human *socs3* promoter (5′-CGATTCCTGGAACTGCGCGG-3′) was used as the probe. (**B**–**G**) Wild-type and mutant STAT3 binding to DNA by modelling. A GAS sequence derived from human *c-fos* promoter (5′-TCGACATTTCCCGTAAATC-3′) was used for modelling. (**B**) Residues H332, R382, F384 and R423 in the DNA binding domain (shown in sphere). (**C**–**G**) Binding model for mutant STAT3 (the carbon is colored magentas, while green is for carbon in wild type STAT3). Hydrogen bond is shown in yellow dash line, and the blue dashed line represents atomic distance.

in STAT3 DNA-binding domain do not exert pronounced effect on Tyr705 phosphorylation of STAT3 (figure 2A). Our results also confirm the important role of the most highly conserved SH2 domain of STAT3 in receptor docking, a process during which gp130 phosphorylated by Jak2 serves as docking site for STAT3 to be phosphorylated by Jak2. Previous work has shown that IL-6 stimulation induces homodimerization of gp130 (Murakami *et al.* 1993) and subsequently leads to the activation of Janus kinases (Jaks) which phosphorylate the tyrosine residues on the receptor cytoplasmic domain of gp130 (Heinrich *et al.* 1998). The 4 C-terminal phosphotyrosine residues (pY) in murine gp130 serve as binding sites for STAT1 and STAT3 (Gerhartz *et al.* 1996). So we suppose that mutations of STAT3 in SH2 domain result in the change of its conformation, affecting its interaction with gp130 and phosphorylation of Tyr705 in response to IL-6. The phosphorylation of both Tyr705 and Ser727 is required for full transcriptional activation of STAT3 (Decker and Kovarik 2000). Serine 727 is reported to be the only phosphoserine site of STAT3 (Wen and Darnell 1997) and both tyrosine and serine phosphorylation are required for full transcriptional activation of STAT3 (Decker and Kovarik 2000; Wen *et al.* 1995). However, unlike that of Tyr705, the phosphorylation of Ser727 is not regulated via SH2 domain of STAT3 in our study (figure 2B). In fact, the phosphorylation status of Ser727 responding to IL-6 are diverse in these mutant STAT3

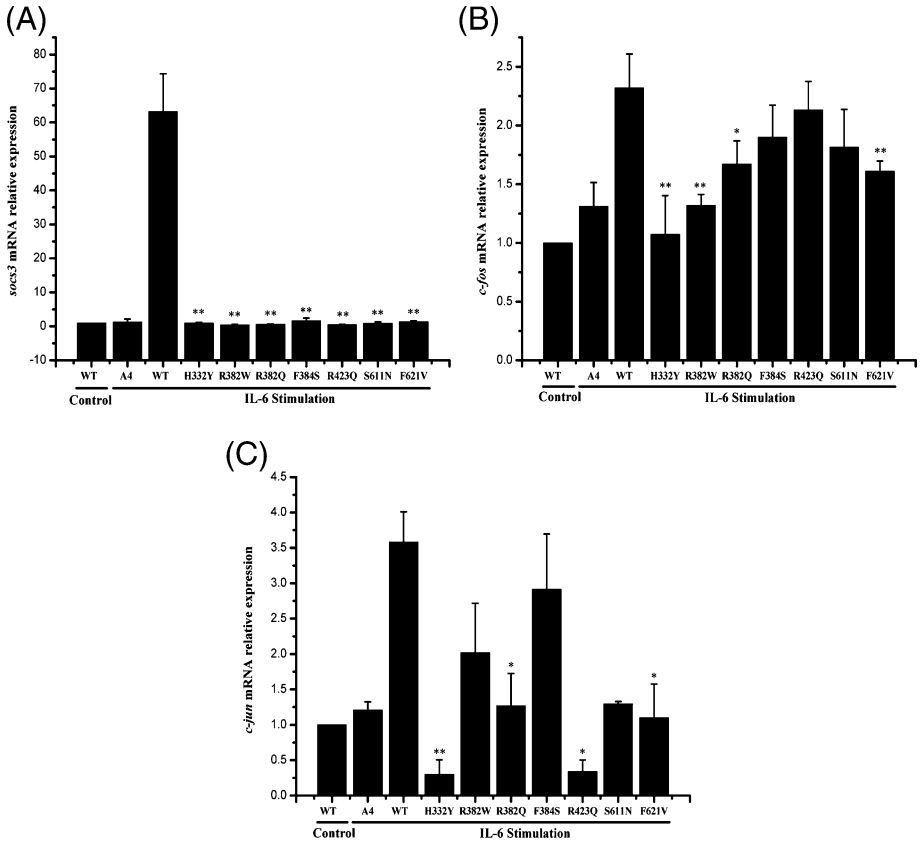

Figure 6. Downstream genes' expression are reduced. (**A**–**C**) Real-Time quantitative PCR for STAT3 target genes. Cells were untreated or stimulated with IL-6 for 2 h, and total RNAs were prepared. Expression of *socs3* (A), *c-fos* (**B**) and *c-jun* (**C**) were examined by real-time PCR. The data shown were normalized to expression of a reference gene GAPDH. Values shown are mean relative expression levels of quadruplicate samples. Error bars are standard deviations. *P<0.05 and **P<0.01 indicate statistically significant differences for comparing stimulated mutant samples with stimulated wild-type sample.

(figure 2B). Combining with the fact that overall phosphorylation status of Ser727 is lower than that of Tyr705 in these mutant cells, we conclude that phosphorylation of Ser727 in STAT3 mutants has not much connection with HIES.

SH2 domain is highly conserved in STAT3 and has been demonstrated to be essential for mediating the dimerization of STATs (Shuai *et al.* 1994). We studied the dimerization of STAT3 in mutants bearing mutation in SH2 domain, as the dimerization ability was reportedly intact between wild-type STAT3 and mutants bearing mutations in DNA-binding domain in response to IFN-α (Minegishi *et al.* 2007). Our work demonstrates that STAT3 mutants with mutations in DNA-binding domain are capable of forming dimers while mutants with mutations in SH2 domain are incapable of doing so in response to IL-6 (figure 3). This finding is consistent with previous work in which a defect in dimerization of STAT3 mutants having mutations in SH2 domain was reported (Kretzschmar *et al.* 2004).

The nuclear importing ability of STAT3 was demonstrated to be independent of either Tyr705 phosphorylation or SH2 domain (Liu *et al.* 2005). In our work STAT3 mutants having mutations in both DNA-binding domain and SH2 domain were distributed in both cytoplasm and nucleus of cells either untreated or treated with IL-6 (figure 4A and B). Western blot analysis shows a little part of Tyr705-phosphorylated H332Y mutant STAT3 is observed in cytoplasm in response to IL-6 (figure 4C). A possible explanation to this phenomenon is that there is relative difficulty of nucleus entrance of Tyr705-phosphorylated H332Y mutation. Interestingly, only H332Y mutation leads to the total transcriptional inhibition of IL-6-induced downstream genes: *socs3*, *c-fos* and *c-jun* (figure 6), consistent with a previous finding of impaired IL-6-induced release of MCP-1 in HIES patients who bear heterozygous mutation of H332Y in STAT3 alleles (Jiao *et al.* 2008). These results, consistent with the previous fact that nuclear entrance signal of STAT3 has been displayed to be in the coiled-coil domain and DNA-binding domain (Liu *et al.* 2005; Ma *et al.* 2003), indicate that amino acid change from histidine (H) to tyrosine (Y) at amino acid position 332, which locates between coiled-coil domain and DNA-binding domain of STAT3, probably affects the nucleus importing ability of Tyr705-phosphorylated STAT3 to a certain extent.

The dominant-negative effects of mutant STAT3 on wild-type STAT3, which leads to the diminishment of DNA-binding ability of STAT3 dimer, have been identified as the major cause of HIES (Minegishi *et al.* 2007). However, the DNA-binding ability of mutant STAT3 identified in HIES patients needs to be elucidated. Our data critically demonstrate that H332Y, R382W, R382Q, F384S, R423Q, S611N and F621V mutant STAT3 are unable to bind to the target DNA sequences (figure 5A). As a novel mutation in DNA-binding domain of STAT3, H332Y mutation was suggested to be disease causing (Jiao *et al.* 2008). The importance of His332 in DNA-binding of STAT3 is clearly demonstrated in a previous study on the three-dimensional structure of STAT3 bound to DNA (Becker *et al.* 1998). In our study, both DNA-binding assay (figure 5A) and transcriptional regulation assay (figure 6) show a total incapacity for H332Y mutation. According to molecular modelling, this DNA binding incapacity of mutant H332Y is caused by a lost hydrogen bond and decreased electrostatic interaction with DNA base DC1010 (figure 5C). Previous bioinformatics analysis predicted the human polymorphisms from Arg (R) to Trp (W) or to Gln (Q) to affect protein function (Ng and Henikoff 2002). In HIES patients, STAT3 mutations in R382W and R382Q have been identified as two hot spots for causing disease (Holland *et al.* 2007) and have been manifested to reduce DNA-binding ability of wild-type STAT3 because of the dominant-negative effect (Minegishi *et al.* 2007). In our study, both R382W and R382Q mutant STAT3 totally lose the DNA-binding ability (figure 5A). $\Delta\Delta G_{kd}$ is 0.82 kcal/mol and 1.64 kcal/mol for R382W and R382Q mutant STAT3 respectively, and we find that the electrostatic interaction between WT-STAT3 H332 and DNA DT 1006 is greatly decreased by these two mutants (figure 5D and E). There are differences between EMSA assay and molecular modeling in F384S mutation and R423Q mutations. This is because we used GAS element from *socs3* promoter as probe for EMSA assay, while in molecular modelling we used GAS sequence from *c-fos* promoter as binding sequence. EMSA assay shows that both F384S and R423Q STAT3 can hardly bind to the target sequence (figure 5A) while molecular modelling for mutation F384S shows that $\Delta\Delta G_{kd}$ is −0.09 kcal/mol, which means that this mutant STAT3 has similar DNA binding capacity as that of wild-type STAT3. Although the distance between F384 and DT1006 is 5.3 Å, showing almost no binding contributed by F384 (figure 5F), $\Delta\Delta G_{kd}$ (R423Q) is −0.22 kcal/mol, which means R423Q mutant STAT3 binding to DNA is stronger than wild-type STAT3. Polar solvation costs a little more energy for R423 binding to DNA ($\Delta\Delta G_{solP}$ is −0.24 kcal/mol), which means R423Q mutation still maintains its DNA-binding ability. These are consistent with our downstream genes' expression assays (figure 6). F384S and R423Q fail to induce expression of *socs3* (figure 6A), while they still have the ability to induce expression of *c-fos* in a certain extent (figure 6B). S611N, F621V and V637M mutations were identified as three hot spots for causing HIES in the SH2 domain of STAT3 (Holland *et al.* 2007), and the defective phosphorylation on Tyr705 residue of V637M mutation has been well documented (Renner *et al.* 2008). In our study, both S611N and F621V mutations exert defective phosphorylation on Tyr705 residue (figure 2A) and incapacity of dimerization (figure 3) as well as total loss of DNA-binding ability

(figure 5A), suggesting the important role of SH2 domain. It has been demonstrated that STAT1 plays a key role in promoting apoptosis in a variety of cell types whereas STAT3 has an anti-apoptotic effect (Stephanou and Latchman 2005), although Tyr701-phosphorylated STAT1 could form a hetero-dimer with STAT3 and the reciprocal regulation of STAT1 and STAT3 activation happens (Regis *et al.* 2008; Schindler and Darnell 1995). However, in our assay (figure 5A) STAT3/STAT1 hetero-dimer is not detected. A reasonable explanation to this phenomenon is the overexpression level of STAT3 is much more than the expression of STAT1, which makes STAT3/STAT3 homo-dimer be the most form in response to IL-6. Moreover, our study shows a homo-dimer formation of STAT1 in A4 cell line in response to IL-6, which is consistent with previous finding that STAT1 can be activated efficiently by IL-6 when STAT3 is absent (Costa-Pereira *et al.* 2002). Interestingly, Line 8 shows that homo-dimer of STAT1 also maintains higher affinity to GAS sequence and Line 6 and Line 9 show lower affinity of STAT1 homo-dimer to GAS sequence, while STAT1 homo-dimer can hardly be detected in other lines (figure 5A).

Quite a number of genes were documented as STAT3 target genes, including *socs3*, *c-fos*, *c-jun*, *c-myc* and *bcl-xl*. To study the transcriptional ability of STAT3 mutants, we selected *socs3*, *c-fos* and *c-jun* in evaluation of the expression pattern. *Socs3* is induced rapidly by IL-6 via STAT3-dependent pathway and its mRNA expression is indicative of transcriptional activity of STAT3 (Starr *et al.* 1997; Yu *et al.* 2009). Our results show that all the STAT3 mutants fail to induce *socs3* mRNA expression, indicating that STAT3 mutations correlated with HIES lose their transcriptional activities on some target genes in this scenario (figure 6A). As components of transcription factors AP-1, c-Fos and c-Jun have been reported to be up-regulated by IL-6 and TPA via the mitogen-activated protein kinase (MAPK) pathway (Schuringa *et al.* 2001). Interaction between STAT3 and c-Jun for inducing transcription on some STAT3 target genes has been well documented (Ginsberg *et al.* 2007). In our study, variations in the expression patterns of *c-fos* and *c-jun* have been clearly displayed for the STAT3 mutants (figure 6B and C). Mutations in R382W, R382Q, F384S, R423Q, S611N and F621V show retaining of comparable ability to transcribe *c-fos*, while mutation in H332Y almost loses the ability to transcribe *c-fos* (figure 6B). On the other hand, mutations in H332Y and R423Q show loss in ability to induce expression of *c-jun*, whereas mutations in R382W and F384S have retained the comparable abilities, and mutations in R382Q, S611N and F621V almost lose the ability to transcribe *c-jun* (figure 6C). Furthermore, the reduced transactivation of STAT3 on ROR-γ mRNA was found to be directly related to the STAT3 mutations in HIES patient's cells and resulted in the abnormal differentiation and deficient production of Th17 cells, which if deficient, subject the HIES patients to bacterial infection (Happel *et al.* 2005; Ma *et al.* 2008). Our result showing an aberrant transactivation of STAT3 mutants on *socs3*, *c-fos* and *c-jun* opens a possibility of more aberrant expression of other STAT3 targets genes to be identified and necessitates the characterization of STAT3 target genes in STAT3-mutation-positive HIES patients' cells.

In summary, in the present study we focused on the functional loss of STAT3 caused by single mutations clinically identified and correlated with HIES. We generated with the STAT3-null A4 cells seven mutants of STAT3 bearing single mutation in the DNA-binding domain and SH2 domain and studied the IL-6-JAK/STAT3 signalling transduction in these mutants. It could be concluded from our study that mutations of STAT3 that are correlated with HIES have impaired the IL-6-Jak/STAT3 signalling pathway by exerting their differing effects on the phosphorylation and dimerization of STAT3, interaction between STAT3 and target DNA sequences, and critically affecting the transactivation of target genes. Since the HIES is a complex genetic disease that may involve a major signalling network, characterization of Jak/STAT3 signalling pathway is far from a mechanistic understanding of HIES but substantially rewarding. In the future, therapy targeting Jak/STAT3 signalling is expected for HIES patients.

Acknowledgements

This work was supported by grants NCET-08-0260 from Ministry of Education and 2009DFA30990 from Ministry of Science and Technology of the People's Republic of China; 0708WCGA149 from the Gansu Provincial Science and Technology to JY.

References

Al Khatib S, Keles S, Garcia-Lloret M, Karakoc-Aydiner E, Reisli I, Artac H, Camcioglu Y, Cokugras H, *et al.* 2009 Defects along the T(H)17 differentiation pathway underlie genetically distinct forms of the hyper IgE syndrome. *J. Allergy Clin. Immunol.* **124** 342–348, 348 e341–345

Avery DT, Ma CS, Bryant VL, Santner-Nanan B, Nanan R, Wong M, Fulcher DA, Cook MC and Tangye SG 2008 STAT3 is required for IL-21-induced secretion of IgE from human naive B cells. *Blood* **112** 1784–1793

Becker S, Groner B and Muller CW 1998 Three-dimensional structure of the Stat3beta homodimer bound to DNA. *Nature* **394** 145–151

Buckley RH, Wray BB and Belmaker EZ 1972 Extreme hyperimmunoglobulinemia E and undue susceptibility to infection. *Pediatrics* **49** 59–70

Costa-Pereira AP, Tininini S, Strobl B, Alonzi T, Schlaak JF, Is'harc H, Gesualdo I, Newman SJ, *et al.* 2002 Mutational switch of an IL-6 response to an interferon-gamma-like response. *Proc. Natl. Acad. Sci. USA* **99** 8043–8047

Darnell JE, Jr. 1997 STATs and gene regulation. *Science* **277** 1630–1635

Darnell JE, Jr., Kerr IM and Stark GR 1994 Jak-STAT pathways and transcriptional activation in response to IFNs and other extracellular signaling proteins. *Science* **264** 1415–1421

Davis SD, Schaller J and Wedgwood RJ 1966 Job's Syndrome. Recurrent, "cold", staphylococcal abscesses. *Lancet* **1** 1013–1015

Decker T and Kovarik P 2000 Serine phosphorylation of STATs. *Oncogene* **19** 2628–2637

Freeman AF and Holland SM 2010 Clinical manifestations of hyper IgE syndromes. *Dis. Markers* **29** 123–130

Freeman AF, Kleiner DE, Nadiminti H, Davis J, Quezado M, Anderson V, Puck JM and Holland SM 2007 Causes of death in hyper-IgE syndrome. *J. Allergy Clin. Immunol.* **119** 1234–1240

Gerhartz C, Heesel B, Sasse J, Hemmann U, Landgraf C, Schneider-Mergener J, Horn F, Heinrich PC and Graeve L 1996 Differential activation of acute phase response factor/STAT3 and STAT1 via the cytoplasmic domain of the interleukin 6 signal transducer gp130. I. Definition of a novel phosphotyrosine motif mediating STAT1 activation. *J. Biol. Chem.* **271** 12991–12998

Ginsberg M, Czeko E, Muller P, Ren Z, Chen X and Darnell JE Jr 2007 Amino acid residues required for physical and cooperative transcriptional interaction of STAT3 and AP-1 proteins c-Jun and c-Fos. *Mol. Cell Biol.* **27** 6300–6308

Grimbacher B, Holland SM, Gallin JI, Greenberg F, Hill SC, Malech HL, Miller JA, O'Connell AC and Puck JM 1999a Hyper-IgE syndrome with recurrent infections–an autosomal dominant multisystem disorder. *New Engl. J. Med.* **340** 692–702

Grimbacher B, Holland SM and Puck JM 2005 Hyper-IgE syndromes. *Immunol. Rev.* **203** 244–250

Grimbacher B, Schaffer AA, Holland SM, Davis J, Gallin JI, Malech HL, Atkinson TP, Belohradsky BH, *et al.* 1999b Genetic linkage of hyper-IgE syndrome to chromosome 4. *Am. J. Hum. Genet.* **65** 735–744

Guerois R, Nielsen JE and Serrano L 2002 Predicting changes in the stability of proteins and protein complexes: a study of more than 1000 mutations. *J. Mol. Biol.* **320** 369–387

Happel KI, Dubin PJ, Zheng M, Ghilardi N, Lockhart C, Quinton LJ, Odden AR, Shellito JE, *et al.* 2005 Divergent roles of IL-23 and IL-12 in host defense against Klebsiella pneumoniae. *J. Exp. Med.* **202** 761–769

Heinrich PC, Behrmann I, Muller-Newen G, Schaper F and Graeve L 1998 Interleukin-6-type cytokine signalling through the gp130/Jak/STAT pathway. *Biochem. J.* **334** 297–314

Holland SM, DeLeo FR, Elloumi HZ, Hsu AP, Uzel G, Brodsky N, Freeman AF, Demidowich A, *et al.* 2007 STAT3 mutations in the hyper-IgE syndrome. *New Engl. J. Med.* **357** 1608–1619

Jiao H, Toth B, Erdos M, Fransson I, Rakoczi E, Balogh I, Magyarics Z, Derfalvi B, *et al.* 2008 Novel and recurrent STAT3 mutations in hyper-IgE syndrome patients from different ethnic groups. *Mol. Immunol.* **46** 202–206

Kretzschmar AK, Dinger MC, Henze C, Brocke-Heidrich K and Horn F 2004 Analysis of Stat3 (signal transducer and activator of transcription 3) dimerization by fluorescence resonance energy transfer in living cells. *Biochem. J.* **377** 289–297

Liu L, McBride KM and Reich NC 2005 STAT3 nuclear import is independent of tyrosine phosphorylation and mediated by importin-alpha3. *Proc. Natl. Acad. Sci. USA* **102** 8150–8155

Ma CS, Chew GY, Simpson N, Priyadarshi A, Wong M, Grimbacher B, Fulcher DA, Tangye SG and Cook MC 2008 Deficiency of Th17 cells in hyper IgE syndrome due to mutations in STAT3. *J. Exp. Med.* **205** 1551–1557

Ma J, Zhang T, Novotny-Diermayr V, Tan AL and Cao X 2003 A novel sequence in the coiled-coil domain of Stat3 essential for its nuclear translocation. *J. Biol. Chem.* **278** 29252–29260

Milner JD, Brenchley JM, Laurence A, Freeman AF, Hill BJ, Elias KM, Kanno Y, Spalding C, *et al.* 2008 Impaired T(H)17 cell differentiation in subjects with autosomal dominant hyper-IgE syndrome. *Nature* **452** 773–776

Minegishi Y 2009 Hyper-IgE syndrome. *Curr. Opin. Immunol.* **21** 487–492

Minegishi Y, Saito M, Tsuchiya S, Tsuge I, Takada H, Hara T, Kawamura N, Ariga T, *et al.* 2007 Dominant-negative mutations in the DNA-binding domain of STAT3 cause hyper-IgE syndrome. *Nature* **448** 1058–1062

Murakami M, Hibi M, Nakagawa N, Nakagawa T, Yasukawa K, Yamanishi K, Taga T and Kishimoto T 1993 IL-6-induced homodimerization of gp130 and associated activation of a tyrosine kinase. *Science* **260** 1808–1810

Ng PC and Henikoff S 2002 Accounting for human polymorphisms predicted to affect protein function. *Genome Res.* **12** 436–446

Papanastasiou AD, Mantagos S, Papanastasiou DA and Zarkadis IK 2010 A novel mutation in the signal transducer and activator of transcription 3 (STAT3) gene, in hyper-IgE syndrome. *Mol. Immunol.* **47** 1629–1634

Regis G, Pensa S, Boselli D, Novelli F and Poli V 2008 Ups and downs: the STAT1:STAT3 seesaw of Interferon and gp130 receptor signalling. *Semin. Cell Dev. Biol.* **19** 351–359

Renner ED, Rylaarsdam S, Anover-Sombke S, Rack AL, Reichenbach J, Carey JC, Zhu Q, Jansson AF, *et al.* 2008 Novel signal transducer and activator of transcription 3 (STAT3) mutations, reduced T(H)17 cell numbers, and variably defective STAT3 phosphorylation in hyper-IgE syndrome. *J. Allergy Clin. Immunol.* **122** 181–187

Renner ED, Torgerson TR, Rylaarsdam S, Anover-Sombke S, Golob K, LaFlam T, Zhu Q and Ochs HD 2007 STAT3 mutation in the original patient with Job's syndrome. *New Engl. J. Med.* **357** 1667–1668

Schindler C and Darnell JE Jr 1995 Transcriptional responses to polypeptide ligands: the JAK-STAT pathway. *Annu. Rev. Biochem.* **64** 621–651

Schindler C, Levy DE and Decker T 2007 JAK-STAT signaling: from interferons to cytokines. *J. Biol. Chem.* **282** 20059–20063

Schuringa JJ, Jonk LJ, Dokter WH, Vellenga E and Kruijer W 2000 Interleukin-6-induced STAT3 transactivation and Ser727 phosphorylation involves Vav, Rac-1 and the kinase SEK-1/MKK-4 as signal transduction components. *Biochem. J.* **347** Pt 1 89–96

Schuringa JJ, Timmer H, Luttickhuizen D, Vellenga E and Kruijer W 2001 c-Jun and c-Fos cooperate with STAT3 in IL-6-induced transactivation of the IL-6 respone element (IRE). *Cytokine* **14** 78–87

Schymkowitz JW, Rousseau F, Martins IC, Ferkinghoff-Borg J, Stricher F and Serrano L 2005 Prediction of water and metal binding sites and their affinities by using the Fold-X force field. *Proc. Natl. Acad. Sci. USA* **102** 10147–10152

Seidel HM, Milocco LH, Lamb P, Darnell JE Jr, Stein RB and Rosen J 1995 Spacing of palindromic half sites as a determinant of selective STAT (signal transducers and activators of transcription) DNA binding and transcriptional activity. *Proc. Natl. Acad. Sci. USA* **92** 3041–3045

Shuai K, Horvath CM, Huang LH, Qureshi SA, Cowburn D and Darnell JE Jr 1994 Interferon activation of the transcription factor Stat91 involves dimerization through SH2-phosphotyrosyl peptide interactions. *Cell* **76** 821–828

Starr R, Willson TA, Viney EM, Murray LJ, Rayner JR, Jenkins BJ, Gonda TJ, Alexander WS, *et al.* 1997 A family of cytokine-inducible inhibitors of signalling. *Nature* **387** 917–921

Stephanou A and Latchman DS 2005 Opposing actions of STAT-1 and STAT-3. *Growth Factors* **23** 177–182

Wen Z and Darnell JE Jr 1997 Mapping of Stat3 serine phosphorylation to a single residue (727) and evidence that serine phosphorylation has no influence on DNA binding of Stat1 and Stat3. *Nucleic Acids Res.* **25** 2062–2067

Wen Z, Zhong Z and Darnell JE Jr 1995 Maximal activation of transcription by Stat1 and Stat3 requires both tyrosine and serine phosphorylation. *Cell* **82** 241–250

Yang J, Huang J, Dasgupta M, Sears N, Miyagi M, Wang B, Chance MR, Chen X, *et al.* 2010 Reversible methylation of promoter-bound STAT3 by histone-modifying enzymes. *Proc. Natl. Acad. Sci. USA* **107** 21499–21504

Yu H, Pardoll D and Jove R 2009 STATs in cancer inflammation and immunity: a leading role for STAT3. *Nat. Rev. Cancer* **9** 798–809

Zhong Z, Wen Z and Darnell JE Jr 1994 Stat3: a STAT family member activated by tyrosine phosphorylation in response to epidermal growth factor and interleukin-6. *Science* **264** 95–98

MS received 24 October 2011; accepted 13 March 2012

Corresponding editor: SEYED E HASNAIN